Wide-Field Swept-Source Optical Coherence Tomography Analysis of Interocular Symmetry of Choroidal Thickness in Healthy Young Individuals

Min-Su Kim,[1] Hyung-Bin Lim,[1] Woo-Hyuk Lee,[1,2] Kyeung-Min Kim,[1] Ki Yup Nam,[3] and Jung-Yeul Kim[1]

[1]Department of Ophthalmology, Chungnam National University College of Medicine, Daejeon, Republic of Korea
[2]Department of Ophthalmology, Gyeongsang National University College of Medicine, Changwon, Republic of Korea
[3]Department of Ophthalmology, Chungnam National University College of Medicine, Sejong, Republic of Korea

Correspondence: Jung-Yeul Kim, Department of Ophthalmology, Chungnam National University Hospital, #640 Daesa-dong, Jung-gu, Daejeon, 35015, Republic of Korea; kimjy@cnu.ac.kr.

Received: September 11, 2020
Accepted: February 4, 2021
Published: March 3, 2021

Citation: Kim M-S, Lim H-B, Lee W-H, Kim K-M, Nam KY, Kim J-Y. Wide-field swept-source optical coherence tomography analysis of interocular symmetry of choroidal thickness in healthy young individuals. *Invest Ophthalmol Vis Sci.* 2021;62(3):5. https://doi.org/10.1167/iovs.62.3.5

Purpose. The purpose of this paper was to study the bilateral choroidal thickness (CT) symmetry and differences in healthy individuals using wide-field swept-source optical coherence tomography (SS-OCT).

Methods. All participants underwent a wide-field 16-mm 1-line scan using SS-OCT. CTs were measured at the following 12 points: 3 points at 900 µm, 1800 µm, and 2700 µm away from the nasal optic disc margin (nasal peripapillary area), 1 point at the subfovea, 6 points at 900 µm, 1800 µm, and 2700 µm away from the subfovea to the nasal and temporal areas (macular area), and 2 peripheral points at 2700 and 5400 µm from temporal point 3 (peripheral area). Bilateral CTs were measured; their correlations and differences in the corresponding regions were analyzed.

Results. There were no statistically significant differences in CTs between the right and left eyes in all corresponding areas (all $P > 0.05$); they all showed significant positive correlation coefficients (r) (all $P < 0.001$). However, the nasal peripapillary and peripheral areas had relatively low correlation coefficients, compared to the macular areas. In addition, the bilateral CT differences were 32.60 ± 25.80 µm in the macular area, 40.67 ± 30.58 µm in the nasal peripapillary area, and 56.03 ± 45.73 µm in the peripheral area (all $P < 0.001$).

Conclusions. Overall, the CTs of each region were bilaterally symmetrical. However, the differences in CTs increased from the center to the periphery, which indicated that the anatomic variation of the nasal peripapillary and peripheral choroid was greater than that of the macula.

Keywords: choroidal thickness, interocular symmetry, wide-field swept-source optical coherence tomography

The choroid is the vascular layer of the eye, located between the retinal pigment epithelium (RPE) and the sclera. The main function of the choroid is to supply blood and nutrients to the RPE and the outer retina.[1] Other roles include heat dissipation in the macula[2] and the release of scleral growth factors that affect ocular growth.[3,4] Various diseases that are closely related to the choroid have been described, such as age-related macular degeneration,[5,6] central serous chorioretinopathy,[7] polypoidal choroidal vasculopathy,[8] Vogt-Koyanagi-Harada disease,[9] high myopia,[10] birdshot chorioretinopathy,[11] and hypertension.[12] Morphological analysis of the choroid (e.g. thickness, area, or volume) is considered important in patients with these conditions.

Measurement of choroidal thickness (CT) using enhanced depth imaging optical coherence tomography (EDI-OCT) was introduced by Spaide et al.[13] The use of EDI-OCT has enabled imaging of deeper structures (e.g. choroid and choroidoscleral junction) that were difficult to observe in conventional spectral-domain OCT (SD-OCT). However, EDI-OCT has problems, such as light scattering caused by the RPE and choroid.[14] In particular, EDI-OCT is limited in that it is difficult to identify the outer border of the choroid in patients with CT > 500 µm.[15] The recently developed swept-source OCT (SS-OCT) uses a wavelength of 1040 to 1060 µm, which enables deeper penetration. Therefore, SS-OCT can obtain more detailed images of choroid and choroidoscleral junction. These advances in the measurement of CT have made it possible to study the association of CT with various factors, such as age,[16] sex,[17] spherical equivalent (SE),[18] axial length (AL),[19,20] intraocular pressure (IOP).[21]

The scan rate in commercially available SS-OCT is nearly twofold more rapid than conventional SD-OCT. This high scan speed reduces motion artifacts and enables acquisition of wide-field B-scan imaging.[22] Since the introduction of wide-field SS-OCT,[23,24] images of the retina, choroid, and choroidoscleral junctions in the peripheral and macular areas have been obtained without a montage process.[25]

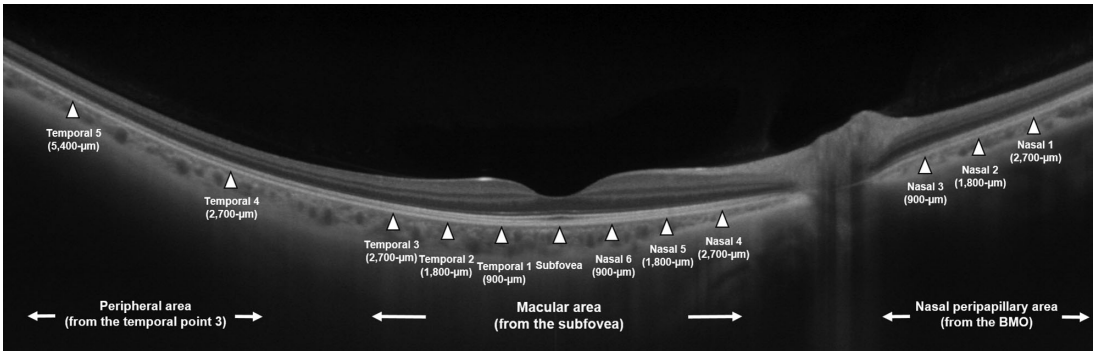

Figure 1. A 16-mm wide-field optical coherence tomography image of a healthy individual. Choroidal thicknesses were measured with a caliper at 12 points as follows; 3 points at 900 μm, 1800 μm, and 2700 μm away from the Bruch's membrane opening (BMO) of nasal optic disc margin (nasal points 3, 2, and 1, respectively; nasal peripapillary area), 1 point at the subfovea, 6 points at 900 μm, 1800 μm, and 2700 μm away from the subfovea to nasal and temporal areas (nasal point 6 and temporal point 1; nasal point 5 and temporal point 2; nasal point 6 and temporal point 3, respectively; macular area), and 2 points at 2700 μm, 5400 μm away from temporal point 3 (temporal points 4, 5, respectively; peripheral area).

Table 1. Baseline Characteristics of Participants

Characteristic		*P* Value
Number of patients (no. of eyes)	32 (64)	N/A
Age, mean ± SD, years	27.75 ± 2.22	N/A
Sex, M/F	19/13	N/A
BCVA, mean ± SD, log MAR*		0.513
Right	0.00 ± 0.16	
Left	−0.01 ± 0.34	
Spherical equivalent, mean ± SD, diopters*		0.613
Right	−3.17 ± 1.90	
Left	−3.08 ± 2.07	
Intraocular pressure, mean ± SD, mm Hg*		0.524
Right	15.97 ± 3.30	
Left	15.81 ± 3.07	
Axial length, mean ± SD, mm*		0.538
Right	24.99 ± 0.90	
Left	24.94 ± 0.91	

* Comparison between right and left eyes using paired *t*-test.
SD, standard deviation; BCVA, best-corrected visual acuity; log MAR, logarithm of the minimum angle of resolution.

Various studies have been conducted regarding peripheral retinal and choroidal morphology using wide-field OCT.[26–28]

In most healthy individuals, both eyes are not anatomically and functionally identical, but they generally appear to be similar. If there is a change in interocular symmetry, the physician should consider whether it is due to disease or constitutes asymmetry within the normal range, as this can have an important effect on the determination of treatment. Understanding interocular symmetry can be an important factor in the diagnosis, treatment, and follow-up of various diseases.

There have been several reports regarding the interocular symmetry of CT.[29–34] However, most studies have focused on CT around the macula. To the best of our knowledge, no study has compared the interocular symmetry of CT in the peripheral area using wide-field SS-OCT. Here, we measured bilateral CTs in the macular, nasal peripapillary, and peripheral areas using a 16-mm wide-field SS-OCT, then analyzed their symmetries and differences.

Methods

This retrospective, observational study was approved by the Institutional Review Board of Chungnam National University Hospital (Daejeon, Republic of Korea). Informed consent was obtained from all participants, and the study protocol adhered to the tenets of the Declaration of Helsinki.

Participants

The study included young healthy adults with no specific findings, all of whom visited the retina clinic in Chungnam National University Hospital for minor ocular discomfort (e.g. dry eye symptoms, floaters, and spectacle prescription due to refractive errors) or regular ophthalmic examination (e.g. evaluation of myopia without discomfort). Age, sex, medical history, and previous ocular surgery information were collected; all patients underwent comprehensive assessments of best-corrected visual acuity (BCVA), IOP (CT-80; Topcon Corporation, Tokyo, Japan), SE (KR-1; Topcon

Investigative Ophthalmology & Visual Science

Table 2. The Reproducibility of Choroidal Thickness Measurements by Different Observers in Both Eyes

		Right Eyes		Left Eyes	
	Points	ICC*	CV	ICC*	CV
Nasal peripapillary area	Nasal 1	0.938	5.22	0.953	4.94
	Nasal 2	0.953	4.91	0.964	5.75
	Nasal 3	0.954	4.87	0.919	6.00
Macular area	Nasal 4	0.975	5.04	0.969	5.12
	Nasal 5	0.987	3.13	0.928	5.91
	Nasal 6	0.957	4.08	0.965	3.91
	Subfovea	0.961	3.44	0.951	3.70
	Temporal 1	0.976	3.03	0.969	3.60
	Temporal 2	0.942	4.68	0.970	4.25
	Temporal 3	0.945	3.98	0.952	3.46
Peripheral area	Temporal 4	0.949	6.03	0.965	5.50
	Temporal 5	0.963	5.23	0.928	4.52

* The P value < 0.05 in all ICC values.
ICC, interclass correlation coefficient; CV, coefficient of variation.

Corporation, Tokyo, Japan), and AL (IOL Master; Carl Zeiss Meditec, Jena, Germany), as well as dilated fundus examinations. SS-OCT (PLEX Elite 9000; Carl Zeiss Meditec, Dublin, CA, USA) was performed to evaluate macular disease and measure CTs.

This study included individuals with a BCVA of 20/20 or better, all of whom had no medical history (e.g. diabetes and hypertension) and no abnormal ocular findings at the comprehensive examinations. Patients with SE < -6.0 D, AL > 26.5 mm, anisometropia > 3.0 D, IOP > 21 mm Hg, chorioretinal disease, glaucoma, optic nerve disease, or previous ocular surgery (including refractive surgery) were excluded.

Image Acquisition

The Zeiss PLEX Elite 9000 instrument is based on SS-OCT and uses a swept-source tunable laser with a center wavelength between 1040 nm and 1060 nm as a light source. In addition, it has a speed of 100,000 A-scans/second and provides an A-scan depth of 3.0 mm in tissue, an optical axial resolution of 6.3 µm in tissue, a digital axial resolution of 1.95 µm in tissue, and a transverse resolution of 20 µm (depending on the beam size at the pupil).

The Zeiss PLEX Elite 9000 instrument offers a variety of scan types; in this study, the HD spotlight 1 (16 mm, 10–100×) scan was used. This scan generates a single, high-definition scan with a depth of 3.0 mm, 100 B-scans, 1024 A-scans, and a length of 16 mm (adjustable to 4, 6, 9, and 12 mm) anywhere on the fundus image. The examiner can set the number of scan frames (scan repetitions) at 10 intervals from 10 to 100. In this study, the HD spotlight 1 scan (with a length of 16 mm and 100 scan frames [repetitions]) was performed twice for all participants by an experienced examiner; the best scan with a signal strength ≥ 9 was selected for analysis. Results from individuals with an OCT scan signal strength < 8 or with a scan artifact were excluded.

CT Measurements

CT measurements were conducted in the manner described in our previous study.[35] In the HD spotlight 16-mm scan, measurements were made at 12 points: 3 points at a distance of 900 µm, 1800 µm, and 2700 µm from the Bruch's membrane opening of nasal optic disc margin (nasal points 3, 2, and 1, respectively; nasal peripapillary area), 1 point at the subfovea, 6 points at a distance of 900 µm, 1800 µm,

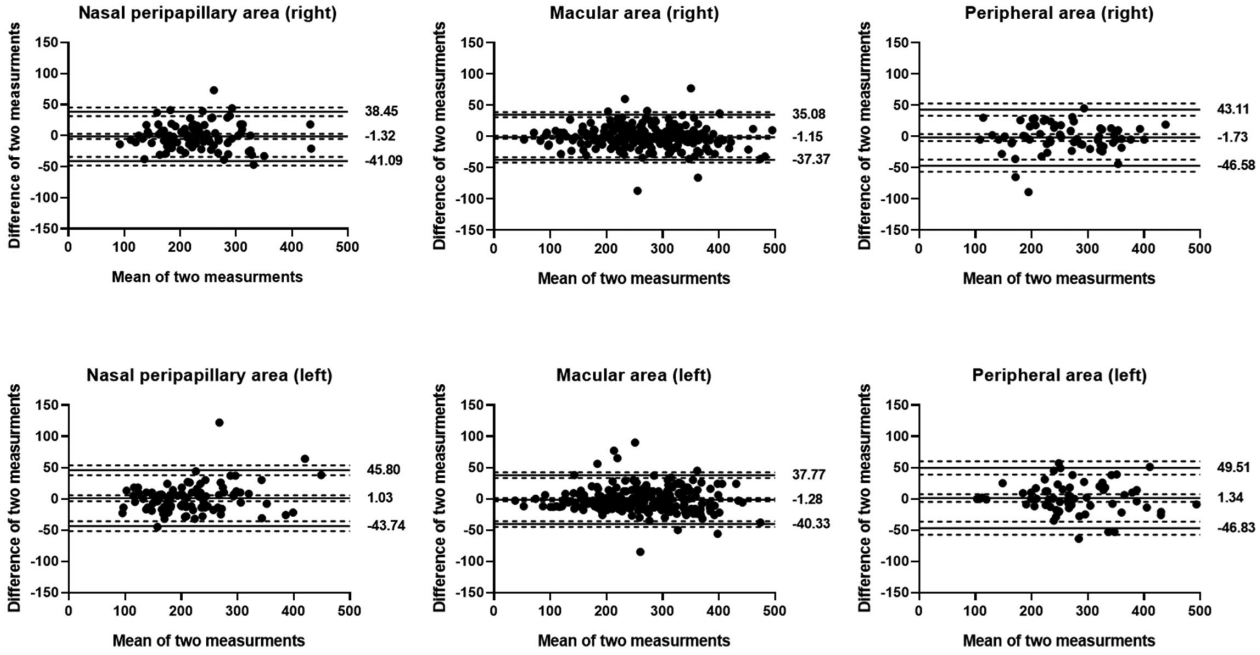

Figure 2. Bland-Altman plots for the agreement of CT measurements between two different observers. The solid lines show the bias (mean of interocular CT difference), upper and lower limits of agreement. The dotted lines represent the 95% confidence interval of the bias, upper and lower limits of agreement. The values of mean bias, upper and lower limits of agreement are shown at the right end of solid lines, respectively. There were no trends according to area or laterality, and the difference in CT measurements by two observers was not significant. CT, choroidal thickness.

Investigative Ophthalmology & Visual Science

Table 3. Comparison of Choroidal Thickness (CT) Measurements Between Right and Left Eyes at Each of 12 Points

		CT, µm, Mean ± SD			Measure of Symmetry		
	Point	Right Eye	Left Eye	*P*- Value*	Interocular Correlation (*r*) (All $P < 0.01$)	ICC (All $P < 0.001$)	CV
Nasal peripapillary area	Nasal 1	243.63 ± 64.83	239.64 ± 69.19	0.675	0.685	0.812	12.50
	Nasal 2	234.02 ± 64.23	220.59 ± 73.09	0.122	0.766	0.863	12.61
	Nasal 3	200.09 ± 56.80	190.44 ± 65.50	0.290	0.665	0.794	15.62
Macular area	Nasal 4	167.69 ± 62.30	171.86 ± 61.48	0.681	0.577	0.732	19.87
	Nasal 5	227.17 ± 76.36	222.67 ± 68.25	0.533	0.850	0.916	10.82
	Nasal 6	276.34 ± 81.37	261.59 ± 70.48	0.159	0.909	0.947	7.79
	Subfovea	299.92 ± 70.87	295.94 ± 68.32	0.569	0.842	0.914	7.59
	Temporal 1	297.13 ± 66.54	294.91 ± 68.08	0.647	0.919	0.958	5.37
	Temporal 2	292.97 ± 62.61	288.69 ± 73.54	0.505	0.873	0.926	7.19
	Temporal 3	309.44 ± 63.69	304.03 ± 59.59	0.549	0.667	0.799	10.23
Peripheral area	Temporal 4	273.44 ± 73.58	294.00 ± 91.92	0.120	0.635	0.765	15.72
	Temporal 5	249.06 ± 79.56	254.84 ± 62.80	0.646	0.530	0.680	16.17

* *P* value for CT measurements in the right and left eyes using the paired *t*-test.
SD, standard deviation; *r*, Pearson's correlation coefficient; ICC, interclass correlation coefficient; CV, coefficient of variation.

and 2700 µm from the subfovea to the nasal and temporal areas (nasal point 6 and temporal point 1, nasal point 5 and temporal point 2, and nasal point 6 and temporal point 3, respectively; macular area), and 2 points at a distance of 2700 µm, and 5400 µm from the temporal point 3 (temporal points 4 and 5, respectively; peripheral area; Fig. 1). The interval between one point and another point was defined as the distance between two points on the hyper-reflective line (corresponding to the RPE-Bruch's membrane complex), not the choroidoscleral junction. After drawing a line in the tangential direction from the hyper-reflective line of each point, the choroidal thickness was measured from the outer portion of the hyper-reflective line to the inner surface of the sclera, using a caliper and built-in review software.

All scans were measured by two investigators (authors K.M.K. and Y.K.W.). Measurement reproducibility was evaluated using the coefficient of variation (CV) and intraclass correlation coefficient (ICC); the mean value of two measurements was used for analysis.

Statistical Analyses

IBM SPSS Statistics for Windows (version 23.0; IBM Corp., Armonk, NY, USA) was used to analyze all data. The paired *t*-test was used to compare BCVA, SE, IOP, AL, and CTs between the right and left eyes. Bland-Altman plots were made to determine the reproducibility of CT measurement by two different investigators, and to compare CT measurements between the right and left eyes. Pearson's correlation coefficient (r), ICC, and CV values were obtained to determine the symmetry of CTs. The absolute values of difference were used to compare differences in bilateral CT measurements at the corresponding regions. One-way analysis of variance (ANOVA) and Bonferroni correction were used to compare interocular differences among the nasal peripapillary, macular, and peripheral areas. Linear regression analysis was used to analyze relationships between interocular differences of CT and clinical factors in nasal peripapillary, macular, and peripheral areas. All values with interocular differences (e.g. SE, IOP, AL, and CT) were analyzed by subtracting left-eye values from right-eye values. A value of $P < 0.05$ was considered statistically significant.

Results

Demographics

This study included 32 participants (19 men and 13 women) with an average age of 27.75 ± 2.32 years. BCVA, SE, IOP, and AL did not significantly differ between the right and left eyes (all $P > 0.05$; Table 1).

Symmetry of Choroidal Thickness by Different Points

CT measurements by two different investigators (authors K.M.K. and Y.K.W.) all showed excellent reproducibility (all ICCs were >0.9 and all CVs were <10%; Table 2, Fig. 2). Table 3 summarizes the mean values of bilateral CT measurements and the interocular symmetry of CTs. Average CT measurements of the right and left eyes in the nasal peripapillary area (nasal points 1, 2, and 3), macular area (nasal points 4, 5, and 6, subfovea, temporal points 1, 2, and 3), and peripheral area (temporal points 4 and 5) showed no statistically significant differences (all $P > 0.05$).

In general, larger ICCs were associated with larger ICC values and smaller CV values; the reverse relationship was also observed. The ICCs of all points in the macular area (except nasal 4 and temporal 3; $r = 0.577$ and 0.667, respectively) were higher than those in the nasal peripapillary area. In addition, the interocular correlation coefficients of all points in the nasal peripapillary area were higher than those in the peripheral area (Table 3, Fig. 3).

Differences in CT Measurements by Points and Area

Table 4 shows the average absolute values of the CT differences between both eyes measured at each of the 12 points. Similar to the results of symmetry, the mean values of CT differences at all points in the macular area (except nasal point 4 and temporal point 3) were smaller than those in the nasal peripapillary area. Furthermore, the mean values of CT differences were smaller at all points in the nasal peripapillary area than at all points in the peripheral area (Fig. 4).

Investigative Ophthalmology & Visual Science

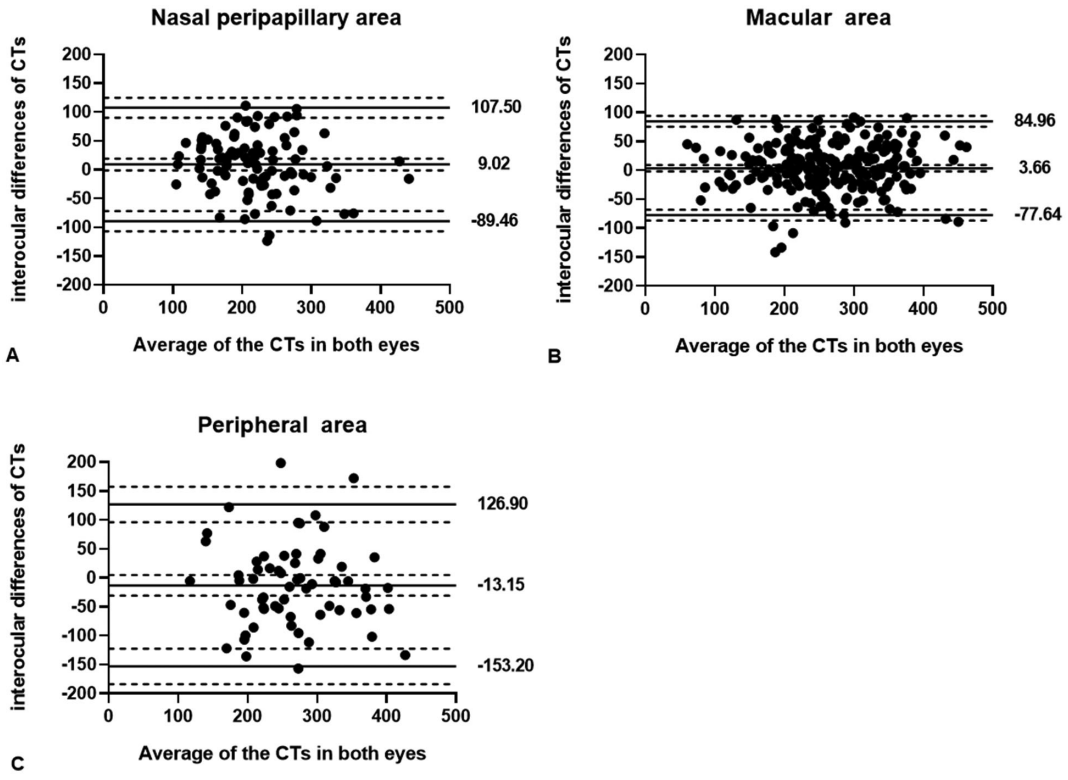

Figure 3. Bland-Altman plots show the agreement between interocular CT measurements in the nasal peripapillary (**A**), macular (**B**), and peripheral (**C**) areas. The solid lines show the bias (mean of interocular CT difference), upper and lower limits of agreement. The dotted lines represent the 95% confidence interval of the bias, upper and lower limits of agreement. The values of mean bias, upper and lower limits of agreement are shown at the right end of solid lines, respectively. Interocular CT differences in the nasal peripapillary area **A** tended to be larger than those in the macular area **B**, and smaller than those in the peripheral area **C**. CT, choroidal thickness.

Table 4. Differences in Choroidal Thickness Measurements (Using Absolute Value) Between Right and Left Eyes at Each of 12 Points

		Differences in Choroidal Thicknesses, µm	
Region		**Mean ± SD**	**95% CI**
Nasal peripapillary area	Nasal 1	41.02 ± 33.51	30.41–52.66
	Nasal 2	39.05 ± 29.80	29.39–48.37
	Nasal 3	41.94 ± 29.17	32.60–52.62
Macular area	Nasal 4	43.27 ± 36.45	31.03–55.90
	Nasal 5	32.65 ± 23.47	24.61–40.86
	Nasal 6	28.53 ± 23.26	21.05–36.30
	Subfovea	31.17 ± 23.43	23.25–38.86
	Temporal 1	22.09 ± 15.49	17.31–27.50
	Temporal 2	27.28 ± 23.22	20.47–35.00
	Temporal 3	43.22 ± 25.39	34.99–52.11
Peripheral area	Temporal 4	57.44 ± 48.07	42.81–74.29
	Temporal 5	56.63 ± 43.98	40.80–69.48

SD, standard deviation; CI, confidence interval.

In the analysis stratified according to area, the mean values of the absolute differences in CT increased gradually in the macular, nasal peripapillary, and peripheral areas (32.60 ± 25.80 µm, 40.67 ± 30.58 µm, and 56.03 ± 45.73 µm, respectively; all $P < 0.001$, 1-way ANOVA). Bonferroni correction showed that the interocular absolute CT differences were smallest in the macular area and largest in the peripheral area (all $P < 0.01$; Table 5).

Clinical Factors Affecting Differences in Interocular CT According to Area

Simple linear regression analysis was performed to analyze the relationships of relative interocular differences (right eyes - left eyes) of CTs in the three different areas (nasal peripapillary, macular, and peripheral areas) with other clinical factors (e.g. age, sex, SE, IOP, and AL; Table 6). BCVA

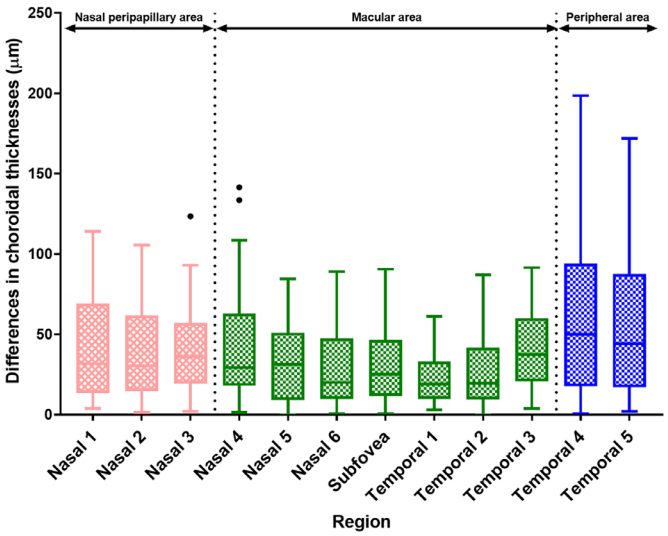

Figure 4. Box plot of absolute interocular differences in CTs according to region. The upper whisker is 75th percentile plus 1.5 times interquartile range, and the lower whisker is 25th percentile minus 1.5 times interquartile range. The outliers are determined to be outside the upper and lower whiskers. CT differences are generally greater in the nasal peripapillary and peripheral areas than in the macular areas. CT, choroidal thickness; Circles, outliers.

Table 5. Comparison of Interocular Differences in Nasal Peripapillary, Macular, and Peripheral Areas

		Region			Statistical Significance	
		Nasal Peripapillary Area	Macular Area	Peripheral Area	*P* Value*	*P* Value†
Differences in CT (μm)	Mean ± SD	40.67 ± 30.58	32.60 ± 25.80	56.03 ± 45.73	<0.001	all <0.01
	95% CI	34.47–46.86	29.20–36.00	44.61–67.45		

* *P* value by one-way analysis of variance among three groups (nasal peripapillary area, macular area, peripheral area).
† *P* value by Bonferroni correction.
CT, choroidal thickness; SD, standard deviation; CI, confidence interval.

was excluded from the analysis because the BCVA logarithm of the minimum angle of resolution was ≤ 0 in all patients included in this study. In terms of macular area, interocular CT differences showed only a significant negative correlation with interocular AL differences ($\beta \pm SD = -24.653 \pm 8.973$ μm/mm, $P = 0.010$), which indirectly indicated that CT and AL were inversely proportional. SE tended to show a weak positive correlation difference, but this was not statistically significant ($\beta \pm SD = 8.382 \pm 4.402$ μm/mm, $P = 0.067$). In the nasal peripapillary and peripheral areas, the difference in CT was not significantly related to any clinical factors (all $P > 0.10$).

Discussion

In this study, bilateral CTs were measured in the macular, nasal peripapillary, and peripheral areas using wide-field SS-OCT; the thicknesses, symmetries, and differences were analyzed at several points. The degree of symmetry was generally high in the macular areas and low in the nasal peripapillary and peripheral areas. Based on the results of symmetry, interocular differences of CTs were inferred to be small in the macular areas and greater in the nasal peripapillary and peripheral areas.

Several studies showed that foveal and parafoveal CTs were thicker in right eyes than in left eyes.[29,30,33,34] Ruiz-Medrano et al.[34] explained that this phenomenon occurred as a result of blood flow variation due to anatomic differences in the right and left carotid arteries. Conversely, a few reports found the CT of the macula was thicker in left eyes than in right eyes.[13,31] The discrepancies among these studies are presumably related to various factors that can influence CT, such as inaccurate measurement, patient demographics (e.g. sex, age, AL, and SE), diurnal variation, and IOP.

Despite the various differences in CTs reported in each paper, most studies[13,29–32] indicated that interocular CTs measured in the foveal and parafoveal areas showed overall high correlation coefficients or ICC values ($r > 0.8$, ICC >0.9). In our study, CTs showed relatively high agreement ($r > 0.8$, ICC >0.9) at the subfoveal, nasal 5, nasal 6, temporal 1, and temporal 2 points, corresponding to the center and inner ring (3-mm diameter centered on the fovea) of the Early Treatment Diabetic Retinopathy Study (ETDRS) map. However, CTs showed relatively low agreement at the nasal 4 and temporal 3 points ($r = 0.577$ and 0.667, respectively), corresponding to the outer ring of the ETDRS map, which differed from the findings in previous reports. In the study by Chen et al.,[30] the correlation coefficient of CT in the temporal area 3 mm from the fovea was 0.490, which was lower than the correlation coefficient of the temporal 3 point (at 2700 μm from the subfovea) in our study. In addition, other reports[36,37] have mentioned the possibility of peripapillary CT variability, which could result from the presence of watershed zones primarily near the optic disc.[38] Therefore,

Table 6. Simple Regression Analysis Comparing Relationships of Clinical Factors With Mean Values of Interocular Differences in CTs, Stratified According to Area

	Simple Regression Analysis, $\beta \pm$ SD					
Area	**Nasal Peripapillary Area**	***P* Value**	**Macular Area**	***P* Value**	**Peripheral Area**	***P* Value**
Age	1.913 ± 3.713	0.611	−0.424 ± 2.206	0.849	0.633 ± 4.798	0.896
Sex (M = 0, F = 1)*	9.509 ± 16.123	0.560	−1.880 ± 8.389	0.824	−28.601 ± 18.598	0.135
Interocular difference						
Intraocular pressure	−3.729 ± 5.865	0.530	3.923 ± 2.927	0.197	3.180 ± 7.010	0.653
Spherical equivalent	−0.128 ± 9.002	0.989	8.382 ± 4.402	0.067	−5.825 ± 10.670	0.589
Axial length	15.001 ± 19.194	0.441	**−24.653 ± 8.973**	**0.010**	20.333 ± 22.795	0.380

All values with interocular differences such as spherical equivalent, intraocular pressure, axial length, and CT were analyzed by subtracting left-eye values from right-eye values.

* Dummy variables for performing regression analysis (19 M and 13 F included in the analysis).

CT, choroidal thickness; SD, standard deviation.

the nasal 4 point showed a very low correlation coefficient compared to the nasal 5 point, which could be attributed to a large variability in CTs due to the watershed zone. The low correlation coefficient of the nasal point 3, compared to nasal point 1 and nasal point 2 within the nasal peripapillary area, may have a similar cause.

To measure the CTs of the nasal peripapillary and peripheral areas, wide-field imaging is required, rather than the modality commonly used in OCT. Several studies have measured peripheral choroidal CTs using wide-field imaging.[35–37,39,40] However, it is difficult to compare CTs with other studies of nasal peripapillary and peripheral areas because CTs were measured at different locations, based on methodological differences. Furthermore, most previous studies included analyses of interindividual variation or topographically intraindividual variation, rather than interocular comparison.[36,37,40] To the best of our knowledge, this is the first study to investigate the interocular symmetry and differences of CTs in the nasal peripapillary and peripheral areas. In this study, the correlation coefficients of CT in the nasal peripapillary and peripheral areas were lower than the correlation coefficient of the macular area (except nasal point 4 and temporal point 3), which objectively demonstrated that the symmetry of the nasal peripapillary and peripheral areas is generally lower than the symmetry of the macular area.

Choroid plays an important role in oxygen supply, and most of the supplied oxygen is consumed by the photoreceptor.[41] Typically, cone cells have the highest density in macular area, and rod cells are mainly in nasal peripapillary and peripheral areas.[42] Assuming that choroidal thickness is associated with oxygen consumption, it can be considered that the interocular symmetry of oxygen consumption in the macular area is greater than that of the nasal peripapillary and peripheral areas. Here, we thought that the distribution of cone cells in the macular area may have a greater interocular symmetry than that of rod cells in the nasal peripapillary and peripheral areas. To date, there have been several studies on the interindividual (person to person) variability of cone and rod cell distribution,[42,43] but there were no studies on intra-individual (interocular) variability. Further study on this will be very interesting. In addition, in our previous study,[35] CT measurements were compared between pachychoroid and normochoroid eyes, using wide-field SS-OCT. Those findings showed that even in normochoroid eyes, pachyvessels were sometimes present in the nasal peripapillary and peripheral areas, which influenced CTs. We presume that this may explain the greater interocular variations (i.e. asymmetries) of the nasal peripapillary and peripheral areas, compared to the macular area.

CT can be affected by various causes, such as age,[16] sex,[17] SE,[18] AL,[19,20] IOP,[21] diurnal variation,[44] and mean arterial pressure.[12] In this study, we also analyzed the relationships of interocular differences of CT with other clinical factors. In the macular area, the interocular CT and AL differences had a significant negative correlation, indicating that the choroid in the macular area becomes thinner as the AL increases, and thicker as the AL decreases. However, in the nasal peripapillary and peripheral areas, there were no significant differences between interocular CTs and ALs. Hoseini-Yazdi et al.[37] analyzed CTs of the macular and extramacular regions in myopic and emmetropic eyes using wide-field EDI-OCT imaging. They reported that CT and AL showed significant negative correlations in macular regions, but no significant relationships in extramacular areas. This finding suggests that AL may have a more important effect on CT in the macular area than in the peripheral area, which is consistent with the results of our study.

Because SE is generally considered to be highly relevant to AL, SE was expected to have a tendency similar to that of AL described above; however, the interocular CT and SE differences tended to show strong trends ($P = 0.067$) in our study. In general, SE is reported to be influenced by factors such as corneal curvature[45] or anterior chamber depth,[46] as well as AL. This may be an important reason for the slightly different results of AL.

Age, sex, and IOP also showed no relationships with interocular CT differences. This is the first study to report relationships of age, sex, and IOP with nasal peripapillary and peripheral CTs. However, only young adults were included in our study, and the age range was narrow (25–35 years; mean age = 27.8 years), which limits the generalizability of the findings. Age is known to be related to CT and further research is needed in this regard, including detailed subgroup analysis.

There were some other limitations in this study. First, CTs were measured manually, which may have led to inaccurate measurements. However, ICC and CV values by the two investigators showed good reproducibility, which might have minimized this problem. Analysis of CT values from automatic measurement software might be useful. Second, the differences in retinal image magnification caused by differences in AL were not considered. AL can affect the transverse scale of the retinal image.[47] Therefore, if the AL of both eyes is different, there is a possibility that each point in the right and left eyes may not be at the same location, and

this may result in measurement error. Further studies using correctly scaled OCT images are needed for this point. Third, because the measured values at each location are related to each other, and both eyes are not independent, the paired *t*-test and absolute difference between the two eyes were used for analysis. Nevertheless, the nonindependency of the measured values may have affected the statistical power. Fourth, vertical SS-OCT scans, including superior and inferior areas, were not included in this study. Finally, we did not analyze other factors, such as mean arterial pressure and diurnal variation, which may affect CT. However, bilateral SS-OCT scans were acquired within 5 minutes. Therefore, we thought that the influence of CTs by mean arterial pressure and diurnal variation could be minimized. Despite these limitations, our study is the first to compare the symmetries and thicknesses of the choroid in the macular, nasal peripapillary, and peripheral areas. In addition, wide-field SS-OCT enabled the images to be captured over a wide range of 16 mm, simultaneously without time lag, thus minimizing errors caused by time differences. Moreover, better image quality and precise CT measurements were obtained in this study, compared to other studies using SD-OCT or EDI-OCT. This study clearly demonstrated that interocular CT variation may be present in the nasal peripapillary and peripheral areas.

In conclusion, interocular CTs generally showed significant symmetries, although there were differences in degree depending on the area. In addition, analysis of the association between interocular CT differences and other clinical factors revealed that only interocular CT and AL differences in the macular area showed meaningful results. This suggests that the interocular CT difference in the nasal peripapillary and peripheral areas is due to anatomic variation alone, rather than other clinical factors. Physicians should be aware of the possibility of interocular CT differences depending on the area; when a patient exhibits a CT difference beyond the normal limit, it is important to perform detailed examinations to identify any factors or other ophthalmic diseases that might affect CT.

Acknowledgments

Disclosure: **M.S. Kim**, None; **H.-B. Lim**, None; **W.-H. Lee**, None; **K.-M. Kim**, None, **K.Y. Nam**, None; **J.-Y. Kim**, None

References

1. Nickla DL, Wallman J. The multifunctional choroid. *Prog Retin Eye Res*. 2010;29(2):144–168.
2. Parver LM, Auker C, Carpenter DO. Choroidal blood flow as a heat dissipating mechanism in the macula. *Am J Ophthalmol*. 1980;89(5):641–646.
3. Summers Rada JA, Palmer L. Choroidal regulation of scleral glycosaminoglycan synthesis during recovery from induced myopia. *Invest Ophthalmol Vis Sci*. 2007;48(7):2957–2966.
4. Summers JA. The choroid as a sclera growth regulator. *Exp Eye Res*. 2013;114:120–127.
5. Zheng F, Gregori G, Schaal KB, et al. Choroidal thickness and choroidal vessel density in nonexudative age-related macular degeneration using swept-source optical coherence tomography imaging. *Invest Ophthalmol Vis Sci*. 2016;57(14):6256–6264.
6. Gattoussi S, Cougnard-Grégoire A, Korobelnik J-F, et al. Choroidal thickness, vascular factors, and age-related macular degeneration: the ALIENOR Study. *Retina*. 2019;39(1):34–43.
7. Honda S, Miki A, Kusuhara S, Imai H, Nakamura M. Choroidal thickness of central serous chorioretinopathy secondary to corticosteroid use. *Retina*. 2017;37(8):1562–1567.
8. Chung SE, Kang SW, Lee JH, Kim YT. Choroidal thickness in polypoidal choroidal vasculopathy and exudative age-related macular degeneration. *Ophthalmology*. 2011;118(5):840–845.
9. Nakayama M, Keino H, Okada AA, et al. Enhanced depth imaging optical coherence tomography of the choroid in Vogt–Koyanagi–Harada disease. *Retina*. 2012;32(10):2061–2069.
10. Ho M, Liu DT, Chan VC, Lam DS. Choroidal thickness measurement in myopic eyes by enhanced depth optical coherence tomography. *Ophthalmology*. 2013;120(9):1909–1914.
11. Dastiridou AI, Bousquet E, Kuehlewein L, et al. Choroidal imaging with swept-source optical coherence tomography in patients with birdshot chorioretinopathy: choroidal reflectivity and thickness. *Ophthalmology*. 2017;124(8):1186–1195.
12. Akay F, Gundogan FC, Yolcu U, Toyran S, Uzun S. Choroidal thickness in systemic arterial hypertension. *Eur J Ophthalmol*. 2016;26(2):152–157.
13. Spaide RF, Koizumi H, Pozonni MC. Enhanced depth imaging spectral-domain optical coherence tomography. *Am J Ophthalmol*. 2008;146(4):496–500.
14. Hamzah F, Shinojima A, Mori R, Yuzawa M. Choroidal thickness measurement by enhanced depth imaging and swept-source optical coherence tomography in central serous chorioretinopathy. *BMC Ophthalmol*. 2014;14:145.
15. Yamashita T, Yamashita T, Shirasawa M, Arimura N, Terasaki H, Sakamoto T. Repeatability and reproducibility of subfoveal choroidal thickness in normal eyes of Japanese using different SD-OCT devices. *Invest Ophthalmol Vis Sci*. 2012;53(3):1102–1107.
16. Xiong S, He X, Zhang B, et al. Changes in choroidal thickness varied by age and refraction in children and adolescents: a one-year longitudinal study. *Am J Ophthalmol*. 2020;213:46–56.
17. Li XQ, Larsen M, Munch IC. Subfoveal choroidal thickness in relation to sex and axial length in 93 Danish university students. *Invest Ophthalmol Vis Sci*. 2011;52(11):8438–8441.
18. Kim M, Kim SS, Koh HJ, Lee SC. Choroidal thickness, age, and refractive error in healthy Korean subjects. *Optom Vis Sci*. 2014;91(5):491–496.
19. Chalam K, Sambhav K. Choroidal thickness measured with swept source optical coherence tomography in posterior staphyloma strongly correlates with axial length and visual acuity. *Int J Retina Vitreous*. 2019;5:14.
20. Flores-Moreno I, Lugo F, Duker JS, Ruiz-Moreno JM. The relationship between axial length and choroidal thickness in eyes with high myopia. *Am J Ophthalmol*. 2013;155(2):314–319.
21. Usui S, Ikuno Y, Uematsu S, Morimoto Y, Yasuno Y, Otori Y. Changes in axial length and choroidal thickness after intraocular pressure reduction resulting from trabeculectomy. *Clinical Ophthalmol*. 2013;7:1155–1161.
22. Klein T, Huber R. High-speed OCT light sources and systems. *Biomed Optics Express*. 2017;8(2):828–859.
23. Reznicek L, Klein T, Wieser W, et al. Megahertz ultra-wide-field swept-source retina optical coherence tomography compared to current existing imaging devices. *Graefes Arch Clin Exp Ophthalmol*. 2014;252(6):1009–1016.
24. Uji A, Yoshimura N. Application of extended field imaging to optical coherence tomography. *Ophthalmology*. 2015;122(6):1272–1274.

25. McNabb RP, Grewal DS, Mehta R, et al. Wide field of view swept-source optical coherence tomography for peripheral retinal disease. *Br J Ophthalmol*. 2016;100(10):1377–1382.
26. Choudhry N, Golding J, Manry MW, Rao RC. Ultra-widefield steering-based spectral-domain optical coherence tomography imaging of the retinal periphery. *Ophthalmology*. 2016;123(6):1368–1374.
27. Shinohara K, Shimada N, Moriyama M, et al. Posterior staphylomas in pathologic myopia imaged by widefield optical coherence tomography. *Invest Ophthalmol Vis Sci*. 2017;58(9):3750–3758.
28. Kakiuchi N, Terasaki H, Sonoda S, et al. Regional differences of choroidal structure determined by wide-field optical coherence tomography. *Invest Ophthalmol Vis Sci*. 2019;60(7):2614–2622.
29. Al-Haddad C, El Chaar L, Antonios R, El-Dairi M, Noureddin B. Interocular symmetry in macular choroidal thickness in children. *J Ophthalmol*. 2014;2014:472391.
30. Chen FK, Yeoh J, Rahman W, Patel PJ, Tufail A, Cruz LD. Topographic variation and interocular symmetry of macular choroidal thickness using enhanced depth imaging optical coherence tomography. *Invest Ophthalmol Vis Sci*. 2012;53(2):975–985.
31. Orduna E, Sanchez-Cano A, Luesma MJ, Perez-Navarro I, Abecia E, Pinilla I. Interocular symmetry of choroidal thickness and volume in healthy eyes on optical coherence tomography. *Ophthalmic Res*. 2018;59(2):81–87.
32. Yang M, Wang W, Xu Q, Tan S, Wei S. Interocular symmetry of the peripapillary choroidal thickness and retinal nerve fibre layer thickness in healthy adults with isometropia. *BMC Ophthalmol*. 2016;16(1):182.
33. Bhayana AA, Kumawat D, Kumar V, et al. Interocular asymmetry in choroidal thickness in healthy Indian population using swept-source optical coherence tomography. *Indian J Ophthalmol*. 2019;67(7):1252–1253.
34. Ruiz-Medrano J, Flores-Moreno I, Peña-García P, Montero JA, Duker JS, Ruiz-Moreno JM. Asymmetry in macular choroidal thickness profile between both eyes in a healthy population measured by swept-source optical coherence tomography. *Retina*. 2015;35:2067–2773.
35. Lim HB, Kim K, Won YK, Lee WH, Lee MW, Kim JY. A comparison of choroidal thicknesses between pachychoroid and normochoroid eyes acquired from wide-field swept-source OCT [published online ahead of print June 22, 2020]. *Acta Ophthalmologica*, https://doi.org/10.1111/aos.14522.
36. Rasheed MA, Singh SR, Invernizzi A, et al. Wide-field choroidal thickness profile in healthy eyes. *Sci Rep*. 2018;8(1):17166.
37. Hoseini-Yazdi H, Vincent SJ, Collins MJ, Read SA, Alonso-Caneiro D. Wide-field choroidal thickness in myopes and emmetropes. *Sci Rep*. 2019;9(1):3474.
38. Hayreh SS. In vivo choroidal circulation and its watershed zones. *Eye*. 1990;4:273–289.
39. McNabb RP, Grewal DS, Mehta R., et al. Wide field of view of swept-source optical coherence tomography for peripheral retinal disease. *Br J Ophthalmol*. 2016;100(10):1377–1382.
40. Mohler KJ, Draxinger W, Klein T, et al. Combined 60° wide-field choroidal thickness maps and high-definition en face vasculature visualization using swept-source megahertz OCT at 1050 nm. *Invest Ophthalmol Vis Sci*. 2015;56(11):6284–6293.
41. Wangsa-Wirawan ND, Linsenmeier RA. Retinal oxygen: fundamental and clinical aspects. *Arch Ophthalmol*. 2003;121(4):547–557.
42. Curcio CA, Sloan KR, Kalina RE, Hendrickson AE. Human photoreceptor topography. *J Comp Neurol*. 1990;292(4):497–523.
43. Wells-Gray EM, Choi SS, Bries A, Doble N. Variation in rod and cone density from the fovea to the mid-periphery in healthy human retinas using adaptive optics scanning laser ophthalmoscopy. *Eye (Lond)*. 2016;30(8):1135–1143.
44. Tan CS, Ouyang Y, Ruiz H, Sadda SR. Diurnal variation of choroidal thickness in normal, healthy subjects measured by spectral domain optical coherence tomography. *Invest Ophthalmol Vis Sci*. 2012;53(1):261–266.
45. Carney LG, Mainstone JC, Henderson BA. Corneal topography and myopia. A cross-sectional study. *Invest Ophthalmol Vis Sci*. 1997;38(2):311–320.
46. Wong TY, Foster PJ, Ng TP, Tielsch JM, Johnson GJ, Seah SK. Variations in ocular biometry in an adult Chinese population in Singapore: the Tanjong Pagar Survey. *Invest Ophthalmol Vis Sci*. 2001;42(1):73–80.
47. Salmon AE, Sajdak BS, Atry F, Carroll J. Axial scaling is independent of ocular magnification in OCT images. *Invest Ophthalmol Vis Sci*. 2018;59(7):3037–3040.

Investigative Ophthalmology & Visual Science